Progress Report for:

CONTRACTS N00014-96-1-0586 & N00014-97-1-0966

MOVING TARGET DETECTION AND MOTION ESTIMATION IN FOLIAGE USING ALONG TRACK MONOPULSE SYNTHETIC APERTURE RADAR IMAGING

AND

SIGNAL SUBSPACE PROCESSING OF UNCALIBRATED MTD-SARS

Submitted to:

Office of Naval Research
Program Officer William J. Miceli, ONR 3131
Ballston Centre Tower One
800 North Quincy Street
Arlington, VA 22217-5660

Administrative Grants Officer
Office of Naval Research Regional Office Boston
495 Summer Street, Room 103
Boston, MA 02210-2109

Director, Naval Research Laboratory
Attn: Code 2627
4555 Overlook Drive
Washingon, DC 20375-5326

Defense Technical Information Center
8725 John J. Kingman Road
STE 0944
Ft. Belvoir, VA 22060-6218

Distribution Statement:

Approved for public release.

Project Director:

Mehrdad Soumekh
Department of Electrical & Computer Engineering
State University of New York at Buffalo
Amherst, New York 14260
Phone: (716) 645-2422, extension 2138
Fax: (716) 645-3656
Email: msoum@eng.buffalo.edu

Contents

Progress Report:

Moving Target Detection and Motion Estimation in Foliage Using Along Track Monopulse Synthetic Aperture Radar Imaging

AND

Signal Subspace Processing of Uncalibrated MTD-SARs

Mehrdad Soumekh
Department of Electrical & Computer Engineering
State University of New York at Buffalo
Amherst, New York 14260

1a. Overview

This document describes the progress on the work performed for "Moving Target Detection and Motion Estimation in Foliage Using Along Track Monopulse Synthetic Aperture Radar Imaging," under Contract N00014-96-1-0586, and "Signal Subspace processing of Uncalibrated MTD-SARs," under Contract N00014-97-1-0966 for the Office of Naval Research for the period ending on 9/30/97.

The scope of the tasks for this period included the following:

i. Non-overlapping *block-based* implementation of the signal subspace algorithm for moving target detection and Automatic Target Recognition (ATR).

ii. Calibration of wide-beamwidth monopulse SARs.

iii. Overlapping block-based signal subspace processing to estimate target motion parameters.

iv. Application of the signal subspace processing method in other electronic and camera-based imaging systems where the user is interested in calibrating the output of dual sensors, for example, diagnostic medicine and video processing.

1b. Publications

The work has produced the following articles which contain a note on the support from the Office of Naval Research under Contracts N00014-96-1-0586 and N00014-97-1-0966:

M. Soumekh, "Moving target detection in foliage using along track monopulse synthetic aperture radar imaging," *IEEE Transactions on Image Processing*, vol. 6, no. 8, pp. 1148-1163, August 1997.

M. Soumekh, "Signal subspace fusion of uncalibrated sensors with application in SAR, diagnostic medicine and video processing," *Proceedings of IEEE International Conference on Image Processing*, Santa Barbara, October 1997.

2. Background

The along track monopulse SAR imaging system utilizes two radars for its data collection. One radar, Radar 1, is used as a transmitter as well as a monostatic receiver. The other radar, Radar 2, is used only as a bistatic receiver. In our original proposal and [3], we documented a signal processing algorithm of the two monostatic and bistatic databases of the along track monopulse SAR system to obtain two **coherently** identical SAR images of the stationary targets in the scene. While the stationary targets appear the same in the monostatic and bistatic SAR images, however, the same is not true for moving targets.

This fact is the basis for developing a static, which we refer to as the difference image, for Moving Target Detection (MTD). If we denote the monostatic SAR image by $f_m(x,y)$ and the bistatic image by $f_b(x,y)$, the difference image for moving target detection is defined via the following:

$$f_d(x,y) = f_b(x,y) - f_m(x,y).$$

Numerical examples for an anlog track monopulse MTD-SAR system are shown in [3].

These examples correspond to a realistic FOPEN SAR database which is injected with the simulated signatures of four moving targets. For this simulation, the two radars are assumed to be fully calibrated; i.e., there is no relative gain and phase ambiguity in the data collected by the two radars. This idealistic scenario, however, is never encountered in practice. In a realistic monopulse SAR system, the two radars exhibit different amplitude patterns (phase as well as gain) which vary with the radar frequency and the radar position (i.e., the slow-time). Moreover, these amplitude patterns vary from one pulse transmission to another due to heat and other uncontrollable natural factors which affect the internal circuitry of the two radars. These subtle changes of the radars amplitude pattern are difficult to be detected and tracked, and are unknown to the user.

As documented in our earlier progress report and [6], dwWe have develop a theoretical model for the undesirable variations of the amplitude pattern of uncalibrated monopulse radars and their effect in the difference image for MTD. This model indicates that the two monopulse SAR images of a *stationary* target (clutter) are related via

$$f_b(x,y) = f_m(x,y) \ ** \ h(x,y),$$

where $h(x,y)$ is an *unknown* impulse response which depends on the two radars calibration errors [6].

Our proposed signal subspace processing is an algorithm for removing the effect of the calibration ambiguity of the two radars, i.e., $h(x,y)$. The algorithm is also applicable to the general problem of fusion and registration of *uncalibrated* sensors. The general system model is described in the next section.

3. System Model

A classical problem in surveillance with radars or optical sensors, and diagnostic medicine involves examining a scene at various time points or with various sensors, which are located at different aspect angles, and fusing the information of these sensors for image registration, or detecting what we refer to as a *change*. For example, in diagnostic medicine, the image of a biological structure is acquired at different time points, and tested for the presence of irregularities such as a tumor. In surveillance with spaceborne or airborne optical devices, the user utilizes optical images of a scene at different time points to detect changes in, e.g., the environment or the enemy's arsenal. As we mentioned in the previous section, the signals acquired by along track monopulse SARs, which utilize two radars at two different locations (aspect angles), can be used to detect moving targets [3].

A fundamental problem associated with these systems is that the "stationary background" (e.g., the clutter in radar, or the internal organs of the patient in diagnostic medicine) should exhibit the same behavior (signature) when viewed by different sensory systems or at different time points. We refer to this scenario as perfectly *calibrated* sensors. Unfortunately, perfectly calibrated sensors do not exist in practice. In the ideal case of perfectly calibrated sensors, the change in two images can be detected by simply subtracting one image from the other. With uncalibrated sensors, the differencing operation is not practical. This is due to the fact that most of these dual sensory systems seek to detect subtle (weak) changes. Unfortunately, the calibration error's power exceeds a change's power in most practical scenarios.

For the general system model of the above-mentioned problem, we consider a sensory system which acquires one or multidimensional information (snapshots) of a stationary scene at various time points. Our objective is to detect relative change in any two of these snapshots due to the presence of a foreign object (e.g., a moving target in SAR, nonlinear motion in video, or a tumor in a biological structure). For our discussion, we consider two-dimensional snapshots (images). Suppose the image recorded by one sensor is $f_1(x,y)$. Then, the recorded image by the other sensor is modeled via

$$f_2(x,y) \equiv f_1(x,y) \ ** \ h(x,y) + f_e(x,y), \tag{1}$$

where $**$ denotes the two-dimensional convolution. In the above model, $f_e(x,y)$ is the change caused by a foreign object, and $h(x,y)$ is an impulse response which represents the relative shift and blurring in the two images due to slight motion and/or change in the Point Spread Function (PSF) of the two sensors; these two signals, i.e., $f_e(x,y)$ and $h(x,y)$, are unknown. Note that the system model in (1) is the same as the monopulse MTD-SAR system model with $f_1(x,y) = f_m(x,y)$, and $f_2(x,y) = f_b(x,y)$.

The model in (1) states that the output of the second sensor $f_2(x,y)$ is linearly related to the output of the first sensor $f_1(x,y)$ and its shifted versions. There might also be cases

in which the sensors exhibit nonlinearity over time. Moreover, in some applications, the second snapshot could be a linearly-transformed (shifted, rotated and scaled) version of $f_1(x,y)$. One could also develop system models for these scenarios for which the proposed signal subspace method is applicable; see [eqs. (2)-(3), 6]. To present the basic concept behind our work and for notational simplicity, we use the model in (1) in the following discussion. However, the proposed approach can be applied to the more complicated models in [6]; this will be discussed in our numerical results.

If the two sensors were perfectly calibrated, i.e., there was no relative shift and/or change in the PSF of the two sensors, then the impulse response in (1) would be the two-dimensional delta function: $h(x,y) = \delta(x,y)$. In this case, one can detect the presence of the foreign object via the difference of the two images; i.e., $f_d(x,y) \equiv f_2(x,y) - f_1(x,y)$. Our discussion is concerned with scenarios in which the two sensors are not prefectly calibrated. In these problems, a slight relative shift and/or blurring in the PSF of the two sensors yields an error signal which can dominate the foreign object's signature $f_e(x,y)$. (In the SAR, video and medical imaging problems which were cited earlier, $f_e(x,y)$ could be an order of magnitude weaker than $f_1(x,y)$.)

Adaptive filtering methods have been suggested to solve the above problem in one-dimensional cases [2]. To apply these adaptive filtering methods in the two-dimensional problems, consider the discrete measured data in the (x_i, y_j) domain. The impulse response $h(x,y)$ is modeled by a finite two-dimensional discrete filter h_{mn}; the size of the filter, call it (N_x, N_y), is chosen by the user based on a priori information. In the following discussion, we choose both N_x and N_y to be odd integers, and $(n_x, n_y) = (N_x/2-.5, N_y/2-.5)$. Then, the model in (1) is rewritten in the following discrete form

$$f_2(x_i, y_j) = \sum_{m=-n_x}^{n_x} \sum_{n=-n_y}^{n_y} h_{mn}\ f_1(x_i - m\Delta_x, y_j - n\Delta_y) + f_e(x_i, y_j), \tag{2}$$

where (Δ_x, Δ_y) represent the sensor sample spacing in the (x,y) domain. In the adaptive filtering approach, a solution for the impulse response h_{mn} from the knowledge of $f_1(x_i, y_j)$ and $f_2(x_i, y_j)$, call it $\hat{h}_{mn}$, is obtained via minimizing the error function

$$\sum_i \sum_j \mid f_2(x_i, y_j) - \sum_{m=-n_x}^{n_x} \sum_{n=-n_y}^{n_y} \hat{h}_{mn}\ f_1(x_i - m\Delta_x, y_j - n\Delta_y) \mid^2 \tag{3}$$

The resultant solution is used to estimate $f_2(x_i, y_j)$ via

$$\hat{f}_2(x_i, y_j) \equiv \sum_{m=-n_x}^{n_x} \sum_{n=-n_y}^{n_y} \hat{h}_{mn}\ f_1(x_i - m\Delta_x, y_j - n\Delta_y). \tag{4}$$

The statistic used for detecting the foregin object is constructed via $\hat{f}_d(x_i, y_j) \equiv f_2(x_i, y_j) - \hat{f}_2(x_i, y_j)$. In the one-dimensional problems, the solution for $\hat{h}_m$ is formed via computing the inverse of a large covariance matrix, a recursive LMS (gradient descent adaptive) algorithm [2]. These methods may be utilized in the two-dimensional problems via, e.g., *reshaping* the two-dimensional arrays into one-dimensional arrays. This, however, requires processing very large matrices, especially for the covariance matrix and the reshaped discrete filter.

4. Signal Subspace Processing

The signal $\hat{f}_2(x_i, y_j)$ is the projection of $f_2(x_i, y_j)$ into the linear subspace which is defined by $f_1(x_i, y_j)$ and $N-1$, where $N = N_x N_y$, of its shifted versions; i.e.,

$$\Psi \equiv \left[\; f_1(x_i - m\Delta_x, y_j - n\Delta_y);\; m = -n_x, \ldots, n_x,\; n = -n_y, \ldots, n_y \; \right]$$

Thus, it is sufficient to identify the signal subspace Ψ, and then obtain the projection of $f_2(x_i, y_j)$ into this signal subspace to construct $\hat{f}_2(x_i, y_j)$. Let $\psi_\ell(x_i, y_j)$, $\ell = 1, 2, \ldots, N$, be a set of orthogonal basis functions which spans the linear signal subspace of Ψ. To generate this signal subspace, one can use Gram-Schmidt, modified Gram-Schmidt, Householder or Givens orthogonalization procedure. The size of the signal subspace, i.e., N, depends on the user's a priori knowledge of the number of the nonzero coefficients in the discrete model of the impulse response $h(x, y)$. For instance, if the discrete $h(x, y)$ contains (N_x, N_y) nonzero pixels, then we should select $N = N_x N_y$. (A similar assignment/model for $h(x, y)$ is used in the adaptive filtering methods [2].) In practice, the exact value of $N_x N_y$ is not known. In this case, an estimate should be used based on the maximum anticipated degree of shift and calibration errors between the two sensors. In our numerical results, we will show results for different values of (N_x, N_y) for the video and SAR data.

The projection of the $f_2(x_i, y_j)$ into the basis function $\psi_\ell(x_i, y_j)$, which is identified by the series coefficient a_ℓ $(\ell = 1, 2, \ldots, N)$, is found via the following:

$$a_\ell \equiv < \; f_2 \; , \; \psi_\ell \; > = \sum_i \sum_j \; f_2(x_i, y_j) \; \psi_\ell^*(x_i, y_j) \tag{5}$$

The projection of $f_2(x_i, y_j)$ into the signal subspace Ψ is

$$\hat{f}_2(x_i, y_j) \equiv \sum_{\ell=1}^{N} \; a_\ell \; \psi_\ell(x_i, y_j). \tag{6}$$

The signal subspace difference image, i.e., the statistic for detecting the foreign object is $\hat{f}_d(x_i, y_j)$. Note that both the adaptive filtering method in [2] and the signal subspace projection of (5)-(6) seek the same *minimum error energy* solution for the estimate of $f_2(x_i, y_j)$ in the linear subspace of $f_1(x_i, y_j)$ and its shifted versions.

If one desires, the impulse response can be computed via the following procedure. Let $g_k(x_i, y_j)$, $k = 1, \ldots, N$, represent the ordered version of the signals

$$[\ f_1(x_i - m\Delta_x, y_j - n\Delta_y);\ m = -n_x, \ldots, n_x,\ n = -n_y, \ldots, n_y\ ]$$

in the manner the Gram-Schmidt procedure is implemented. We define an N by N matrix $\mathbf{B}$ whose elements are the projection of $g_k(x_i, y_j)$'s into $\psi_\ell(x_i, y_j)$'s; i.e.,

$$b_{k\ell} \equiv < \ g_k \ , \ \psi_\ell \ > = \sum_i \sum_j \ g_k(x_i, y_j)\ \psi_\ell^*(x_i, y_j) \tag{7}$$

Note that $\mathbf{B}$ is a lower triangular matrix since $b_{k\ell} = 0$ for $k < \ell$. We also define the 1 by N vector $\mathbf{A}$ which is made up of the coefficients a_ℓ, $\ell = 1, \ldots, N$, in (5). Using (6) and (7), it can be shown that the following 1 by N vector:

$$\mathbf{H} \equiv \mathbf{A}\ \mathbf{B}^{-1}, \tag{8}$$

contains the estimated impulse response coefficients $\hat{h}_{mn}$.

5. Block-based Processing for MTD and Automatic Target Recognition

As we mentioned earlier, one can develop a model for the undesirable variations of the amplitude pattern of uncalibrated monopulse radars [6, Section IV]. Such a model indicates that the monopulse SAR images are related via $f_b(x, y) = f_m(x, y)\ ** \ h(x, y)$, where $h(x, y)$ is a function of the calibration error of the two radars. This model is the same as the model in (1) with $f_1(x, y) = f_m(x, y)$ and $f_2(x, y) = f_b(x, y)$ for a stationary scene when there is no moving target (foreign object) and, thus, $f_e(x, y) = 0$. Thus, the signal subspace method described in Section 4 can also be applied in the MTD monopulse SAR problem with uncalibrated radars [6].

Provided that the calibration error function is invariant of the target's coordinates, then the subspace processing can be applied in one step to the entire SAR scene. However, in most wide-angle FOPEN SAR systems, the calibration error function cannot be modeled to be invariant of the target's coordinates. In this case, the SAR image has to be divided into subpatches over which the error function does not vary significantly (which implies that $h(x, y)$ approximately remains the same in that subpatch.) The subspace algorithm can then be applied to each subpatch. We refer to this scheme as*block-based* signal subspace processing.

To exhibit the performance of the block-based processing, we consider registration of two SAR images of a foliage or target area in the SAR example of [4]. The two SAR images are reconstructed from two actual separate runs of the aircraft. The following

factors make the two SAR images have different PSF and spatial orientation (shift, scaling and rotation):

i. The aircraft's flight path and altitude slightly vary in the two runs that causes in a relative scaling and rotation of targets in the two SAR images;

ii. The two radars exhibit different amplitude patterns [6];

iii. The two SAR data contain different residual motion errors (even after motion compensation) that results in a fast-time frequency and slow-time (aspect angle) dependent phase error.

Based on the above-mentioned factors and using an analysis similar to the one for the monostatic and bistatic data of a monopulse SAR system [Section IV, 6], one can show that the two SAR images are related via the model [6, eq. (3)].

Figures 1a and 1b show the SAR images of a foliage area for the two radars. Figure 1c and 1d, respectively, are the subspace projection of the (complex) SAR image of Radar 2 into the (complex) SAR image of Radar 1 based on the model (1) and [6, eq. (3)] with $(n_x, n_y) = (4, 4)$. (The signal subspace processing is performed with coherent data, i.e., *complex* SAR images.) Note that Figure 1d is a better representative of the SAR image in Figure 1b. The error (the difference between the SAR image of Radar 2 and its subspace projection) power to the signal power in Figures 8c and 8d are, respectively, -1.2 dB and -6.7 dB.

Figure 2 shows similar results for a truck with $(n_x, n_y) = (2, 2)$. The truck is labeled HEMTT1 in the SAR image of Radar 1 in [5, Figure 2]. Since the slow-time Doppler band of a truck is smaller than that of foliage (see [4],[5]), the size of the filter h_{mn} can be chosen to be smaller in the case of a truck. The error power to the signal power in Figures 2c and 2d are, respectively, -1.7 dB and -6.5 dB.

Figures 3a and 3b are the SAR images of two trucks which are obtained with Radar 1. The two trucks are of the same type but positioned at different coordinates. These trucks are labeled HEMTT1 and HEMTT4 in [5, Figure 2]. Figure 3c and 3d, respectively, are the subspace projection of the SAR image of HEMTT4 into the SAR image of HEMTT1 based on the model (1) and [6, eq. (3)] with $(n_x, n_y) = (2, 2)$. The error power to the signal power in Figures 10c and 10d are, respectively, -3.3 dB and -9.5 dB. The subspace processing based on the model [6, eq. (3)] (Figure 3d) has compensated for the relative change in the orientation of the two trucks as well as the variations of the radar's amplitude pattern in the range and the slow-time domain.

The problem of shift-varying unknown impulse response $h(x, y)$ also arises in other sensor fusion and registration problems. For instance, in medical diagnostic imaging, the CT, MR, ultrasound, etc. images of a patient which are acquired at different time points

do not correspond to the same cross-sectional slices through the patient's body. We have implemented the block-based signal subspace processing on the Magnetic Resonance (MR) images of a patient with Multiple Sclerosis (MS) taken in October 95 (Figure 4a) and March 1996 (Figure 4b). Figure 4c shows the difference image. Figure 4d is the subspace difference image which was formed via block processing.

6. Calibrating Wide-Beamwidth Monopulse SARs

As we showed earlier, the signal subspace processing also provides an estimate of the impulse response $h(x, y)$. In the areas (blocks) of the monopulse SAR images where the subspace difference image $\hat{f}_d(x_i, y_j)$ does not indicate the presence of a moving target, the estimate of the impulse response $h(x, y)$ renders the calibration phase error function of the two monopulse radars. A key challenge here is to fuse the information in the estimated impulse response of the blocks to form a *global* sense of the calibration phase error function; the result can then be used for estimating motion parameters of a detected moving target which is discussed in the next section.

To construct the global calibration phase function versus the slow-time (synthetic aperture) domain, we have considered the calibration phase errors which vary linearly with the fast-time frequency. This class of calibration phase errors are due to the variations of the internal circuitry of the two radars (propagation delays). This type of calibration phase error would be the dominant term in the phase error function between two monopulse SARs. The analytical model for this phase error function is similar to the one which is encountered in SAR motion compensation problems with wide-beamwidth radars.

In this case, the radar distance from a target at (x, y) at the slow-time u is represented via

$$r_{xy}(u) = \sqrt{[x - x_e(u)]^2 + (y - u)^2}, \tag{9}$$

where $x_e(u)$ is a slow-time dependent range error function. In the narrow-beamwidth SAR systems where the target cross-range y and synthetic aperture u values are much smaller than range x, the following approximation is valid:

$$r_{xy}(u) \approx \sqrt{x^2 + (y - u)^2} + x_e(u). \tag{10}$$

Thus, for motion compensation, it is sufficient to multiply the measured SAR signal with the following phase function:

$$\exp\left[\, j2k\; x_e(u) \,\right]. \tag{11}$$

The above approximation-based motion compensation would not work in the FOPEN SAR systems which are intended for MTD in foliage. To show this, we have studied a wide-beamwidth UHF SAR system where the beamwidth is approximately $\pm B = \pm 2000$

meters (P3 data). Figure 5a is the SAR reconstruction in the absence of motion errors for a target located at the cross-range $y = 0$ in this SAR system. Figure 5b shows a simulated motion error function for this system. Figure 5c is the reconstructed target function in the presence of the motion errors of Figure 5b; the target is smeared over a wide cross-range area. Figure 5d is the target reconstruction when the narrow-beamwidth motion compensation in (11) is used. This reconstruction shows smearing of the target due to the narrow-beamwidth approximation in (10) which is not valid in the wide-beamwidth SAR systems.

Consider the target located the cross-range $y = 0$. Due to the narrow-beamwidth approximation, the phase error function in the SAR signature of this target, after the motion compensation of (11), becomes

$$\exp\left[\, j2k\,\sqrt{x^2+u^2} - j2k\sqrt{[x-x_e(u)]^2+u^2} + j2k\; x_e(u)\,\right]. \tag{12}$$

Using the Fourier properties of AM-PM signals, we have shown that the phase error function in (12) translates into the following phase error function in the spatial frequency (k_x, k_y) domain of the target image:

$$\begin{aligned} H(k_x,k_y) = \exp\Big[\, & j\rho\,\sqrt{x^2+U^2(k_x,k_y)} - j\rho\,\sqrt{[x-x_e(u)]^2+U^2(k_x,k_y)} \\ & + j\rho\; x_e[U(k_x,k_y)]\,\Big] \end{aligned} \tag{13}$$

where

$$U(k_x,k_y) = \frac{k_y\; x}{k_x}, \tag{14}$$

and

$$\rho = \sqrt{k_x^2+k_y^2}.$$

Figure 5e shows the target SAR reconstruction in cross-range when the conjugate of the phase error function in (14) is used for motion compensation (after the preliminary narrow-beamwidth motion compensation of (11)). We refer to this as the Fourier-based wide-beamwidth motion compensation. A similar procedure can be used for the targets located at different range and cross-range points. Note that the kernel in (13)-(14) varies with the target's coordinates. Thus, the wide-beamwidth motion compensation is a *shift-varying* operator.

For the MTD monopulse SAR system, the transfer function $H(k_x, k_y)$ is estimated via the signal subspace processing for each block where no moving target is detected. Then, these transfer functions are combined to obtain an estimate the calibration phase error function of the two radars at all slow-time points. The result is then used to remove the calibration phase error function at the blocks where a moving target is detected. The next section describes the block-based processing on the resultant for motion estimation.

7. Block-based Processing for Motion Estimation

After calibrating the monopulse SAR images via the above-mentioned shift-varying motion compensation method, we reapply the signal subspace method at the blocks where a moving target is detected. In this case, the resultant estimate of the impulse response $h(x, y)$ carries information on the motion parameters of the moving target. In the simplest case where the target possesses a constant speed, the estimated impulse response can be shown to indicate a ***shift*** operation; the amount of shift in range and cross-range are proportional to the target's velocity vector. In the case of a target with nonlinear motion, we plan to study a procedure which applies the signal subspace method to the slow-time *subapertures* of the target monopulse SAR signature to estimate the target's *instantaneous* velocity vector.

To examine the merits of the above-mentioned processing for motion estimation, we have applied the signal subspace method to the overlapping blocks of a portion of the video sequence of "Miss America." For our experiment, we used two consecutive frames of Miss America, Frames 15 (Figure 6a), and Frame 16 (Figure 6b). Figure 6c shows the motion vector image which is obtained by the signal subspace processing of these two frames. To form this image, the impulse response $h(x, y)$ is estimated within a 11 by 11 neighborhood of each pixel in the two frames. this corresponds to an *overlapping* block processing. Figures 6d-6g are the close-up images of the estimated motion vector.

8. Future Plans

We plan to continue our investigation on the theoretical and practical aspects of the issues which were discussed in Sections 5-7 (block-based processing for MTD, ATR, and motion estimation). In addition to these, we have identified another relevant problem which might benefit from our investigation of along-track monopulse SARs. The problem is to suppress RF interference in UWB-UHF SAR systems. Our preliminary analytical study has indicated that the data acquired by an along-track monopulse SARs contains valuable information for suppressing RFI. We plan to study this issue further via analytical and numerical means.

REFERENCES

1. B. Cantrell, "A short-pulse area MTI," NRL Report 8162, September 1977.
2. M. Hartless and J. Barry, "Shipboard infrared search and track," Final Report of Contract N66001-94-C-6001, NCCOSC, December 1994.
3. M. Soumekh, "Moving target detection in foliage using along track monopulse synthetic aperture radar imaging," *IEEE Trans. Image Proc.*, vol. 6, no. 8, pp. 1148-1163, Aug. 1997.
4. M. Soumekh, "Reconnaissance with ultra wideband UHF synthetic aperture radar," *IEEE Signal Processing Magazine,* vol. 12, no. 4, pp. 21-40, July 1995.
5. M. Soumekh, "Super-resolution array processing in SAR," *IEEE Signal Processing Magazine*, vol. 13, no. 6, November 1996.
6. M. Soumekh, "Signal subspace fusion of uncalibrated sensors with application in SAR, diagnostic medicine and video processing," *Proc. ICIP*, Santa Barbara, October 1997.

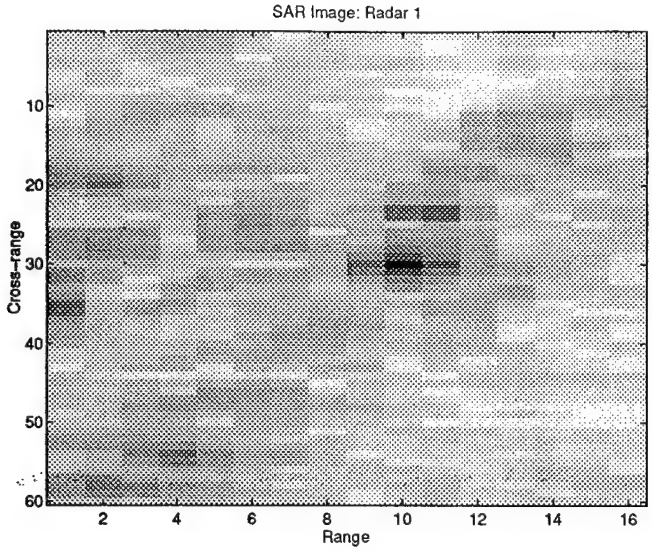

(a)

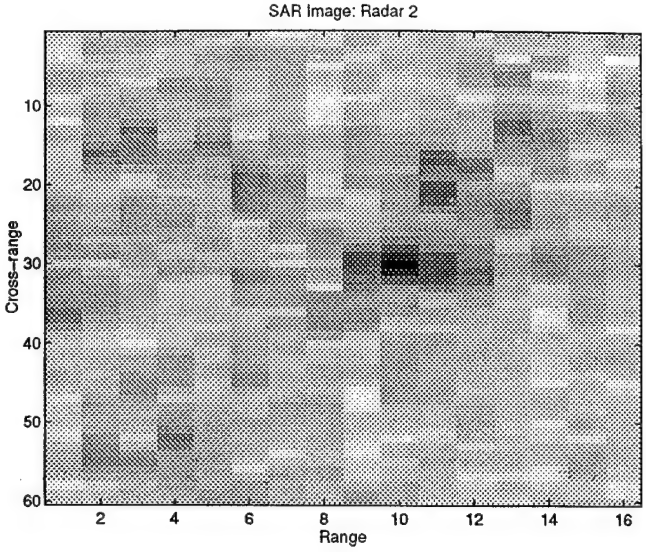

(b)

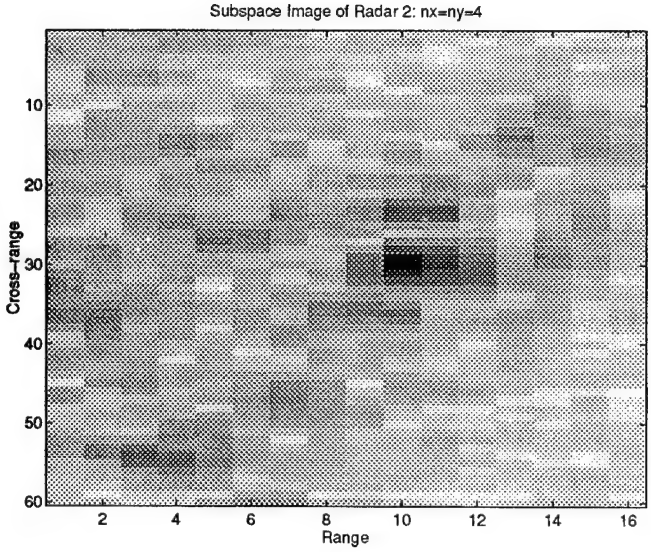

(c)

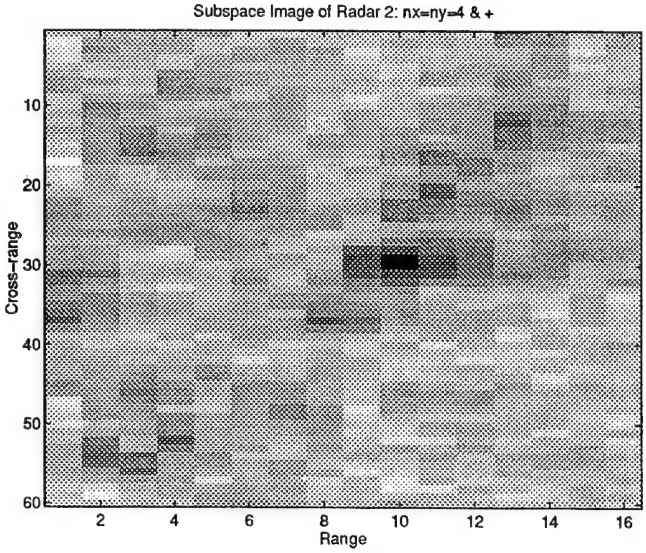

(d)

Figure 1

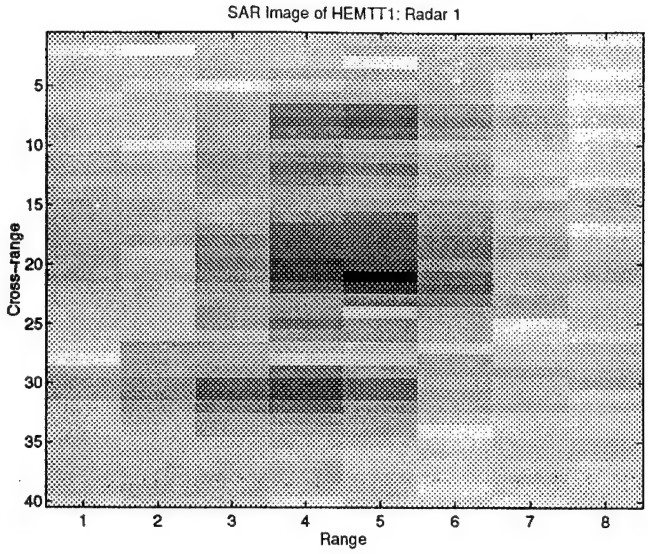

(a)

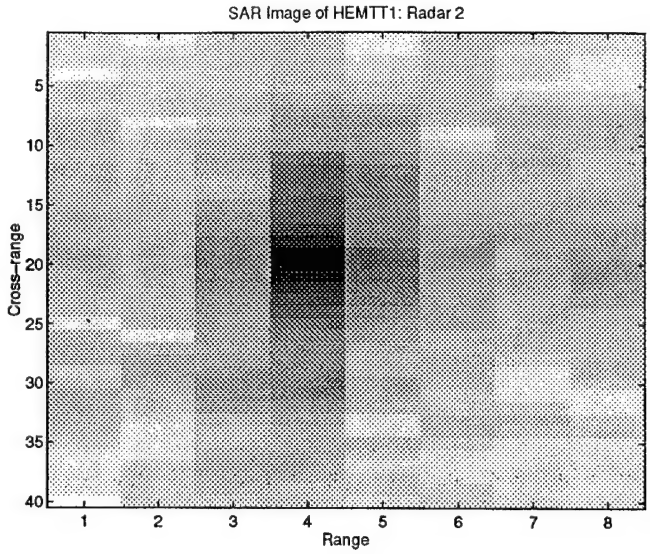

(b)

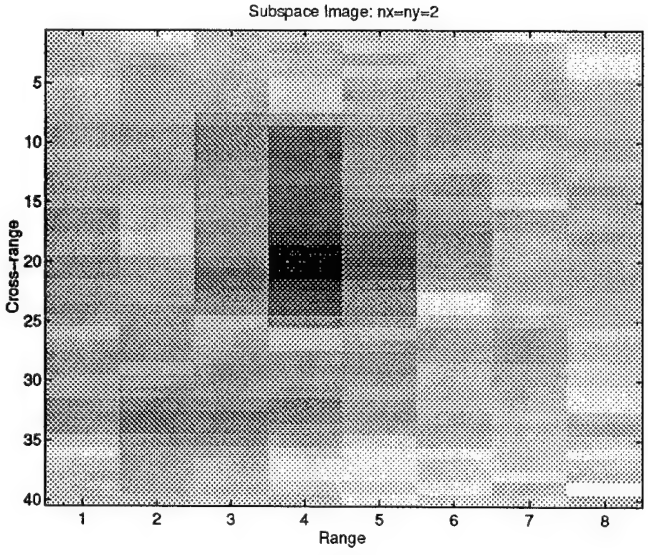

(c)

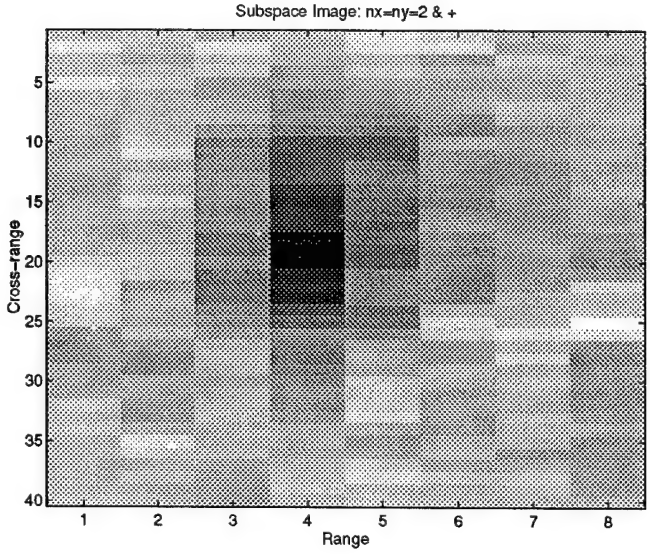

(d)

Figure 2

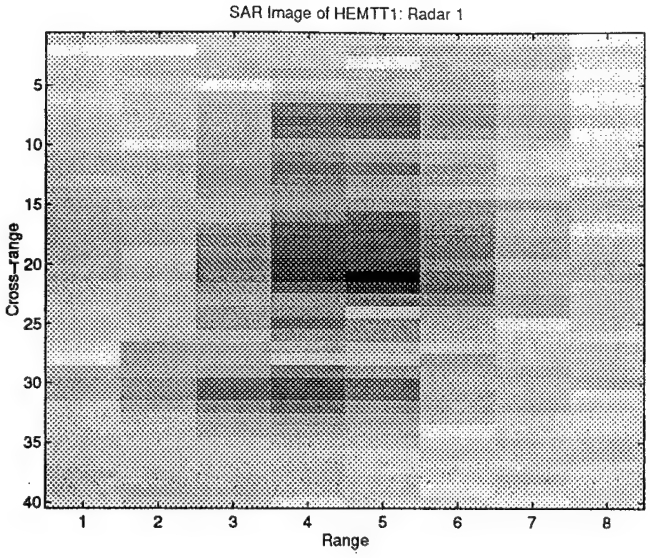

(a)

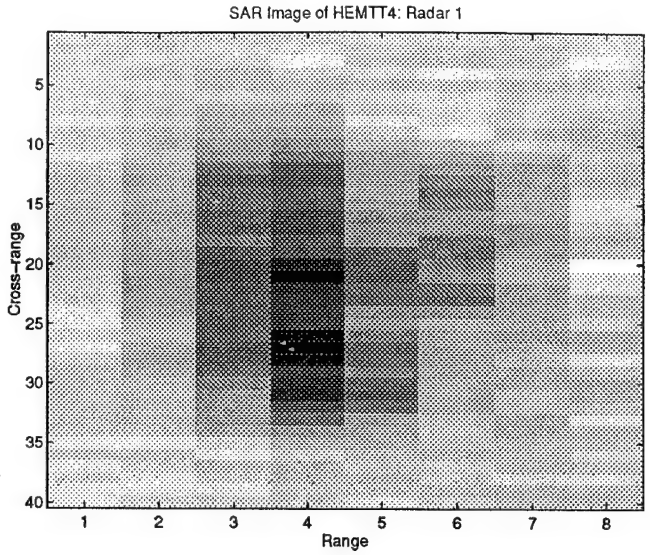

(b)

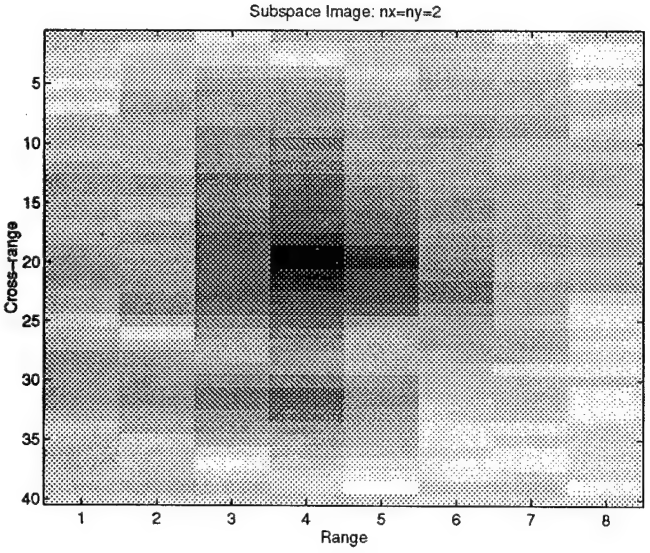

(c)

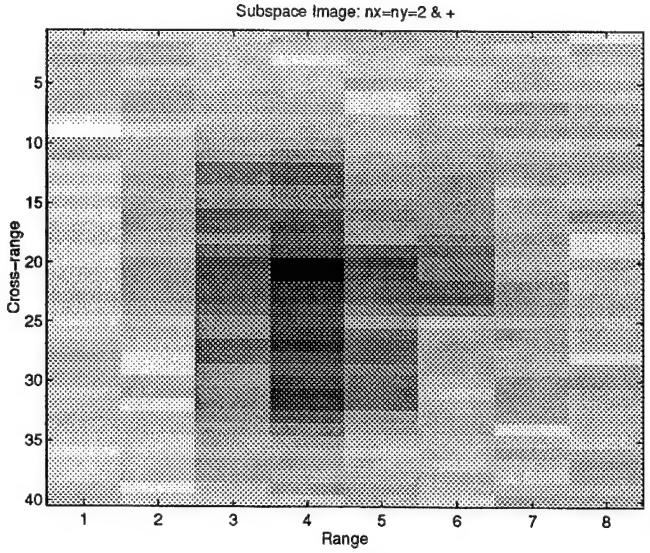

(d)

Figure 3

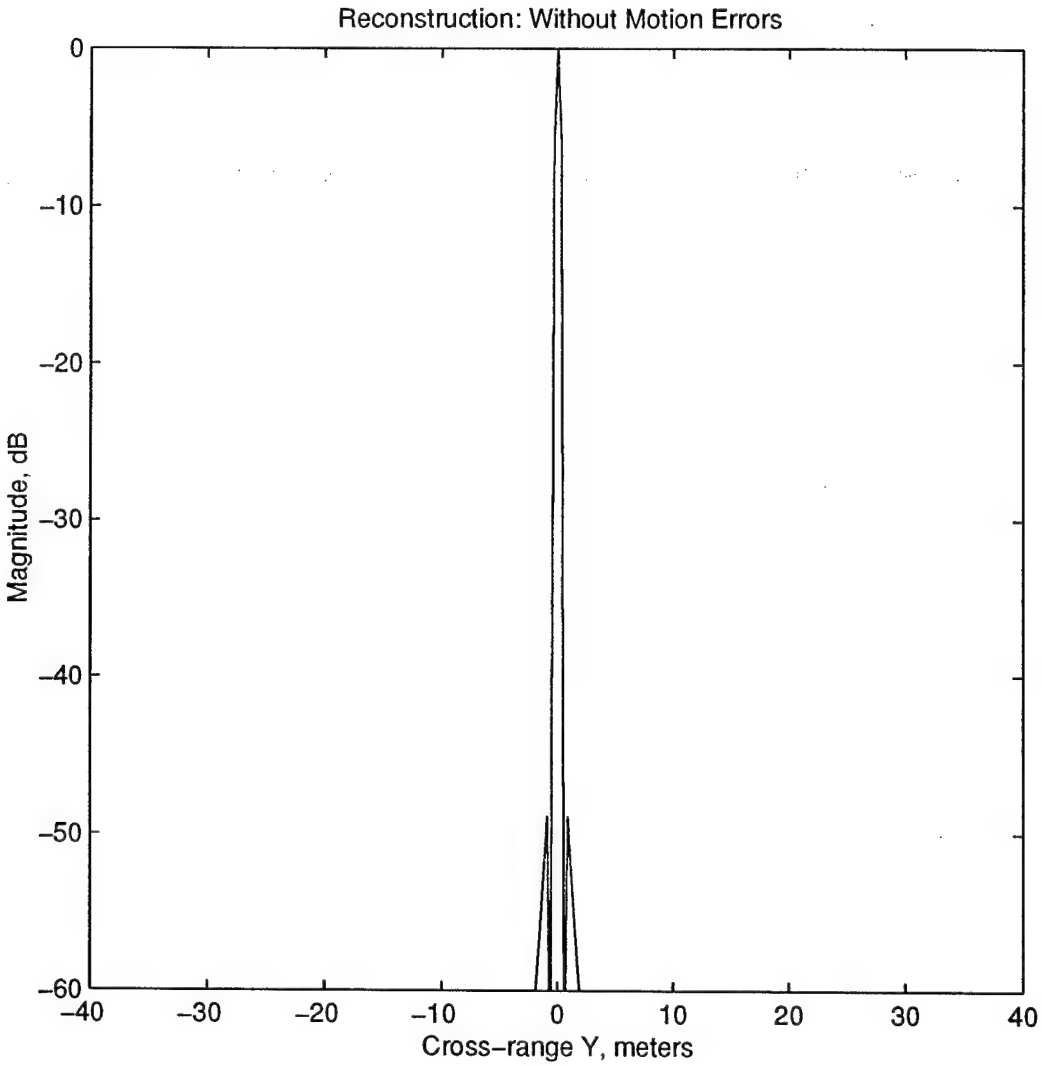
Reconstruction: Without Motion Errors
Magnitude, dB
0
−10
−20
−30
−40
−50
−60
−40
−30
−20
−10
0
10
20
30
40
Cross−range Y, meters

Figure 4a

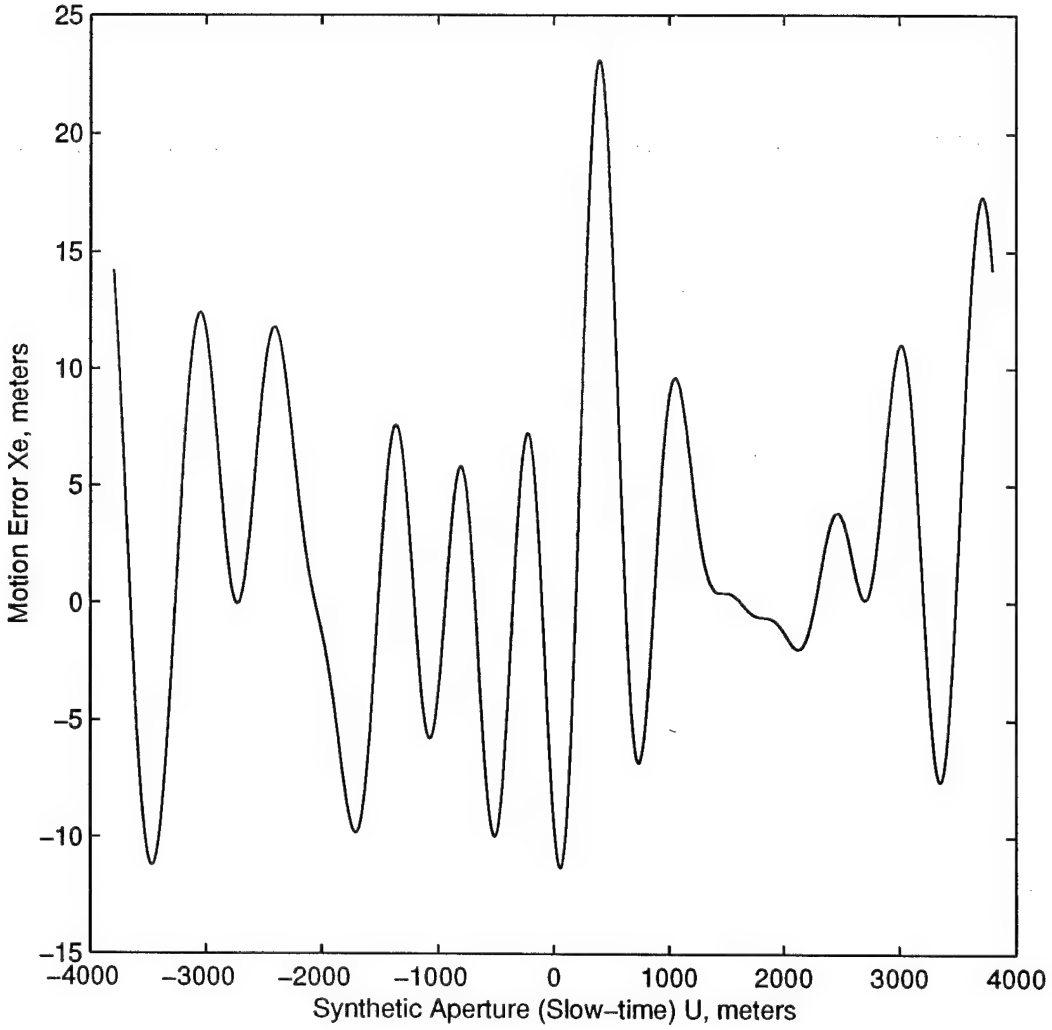
25
20
15
10
5
0
−5
−10
−15
−4000
−3000
−2000
−1000
0
1000
2000
3000
4000
Motion Error Xe, meters
Synthetic Aperture (Slow−time) U, meters

Figure 4b

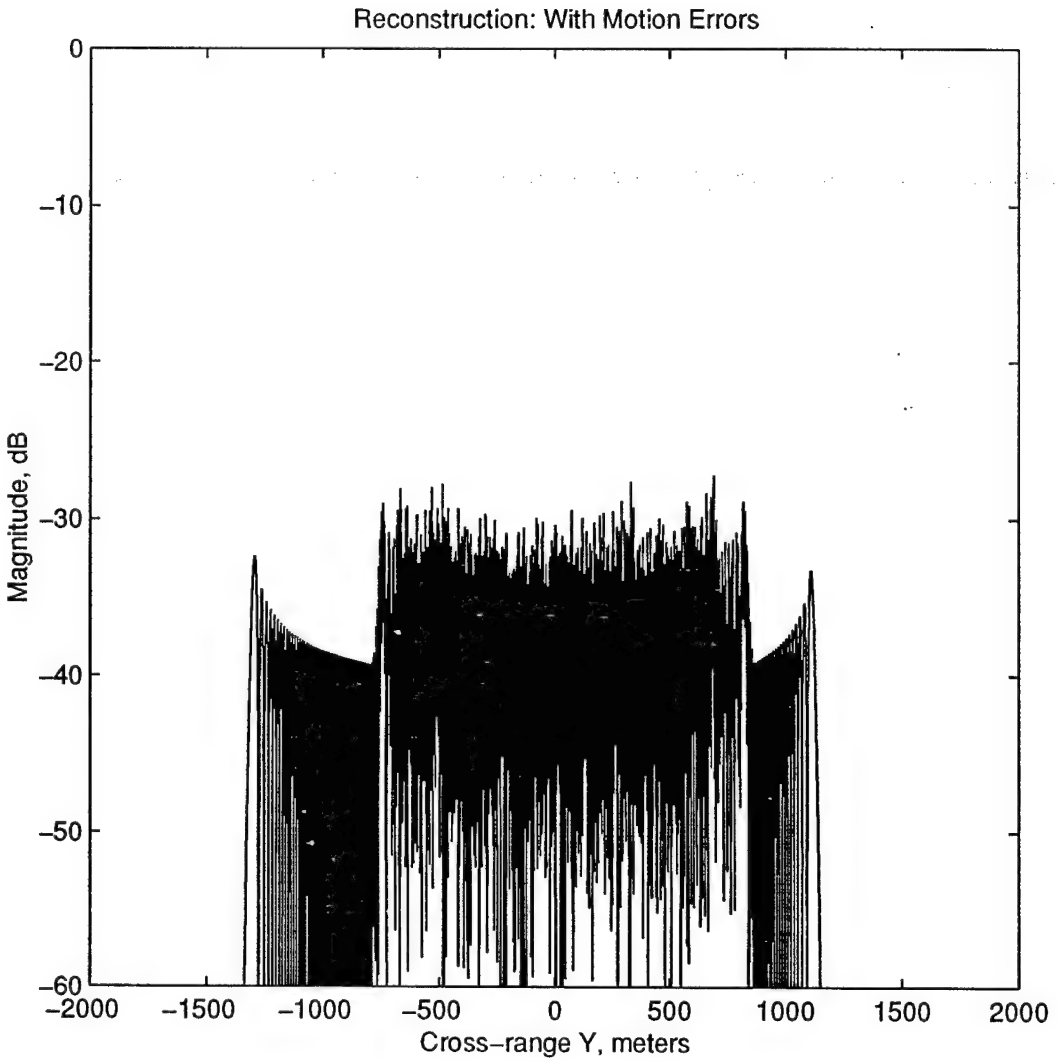
Reconstruction: With Motion Errors
0
−10
−20
−30
−40
−50
−60
Magnitude, dB
−2000
−1500
−1000
−500
0
500
1000
1500
2000
Cross−range Y, meters

Figure 4c

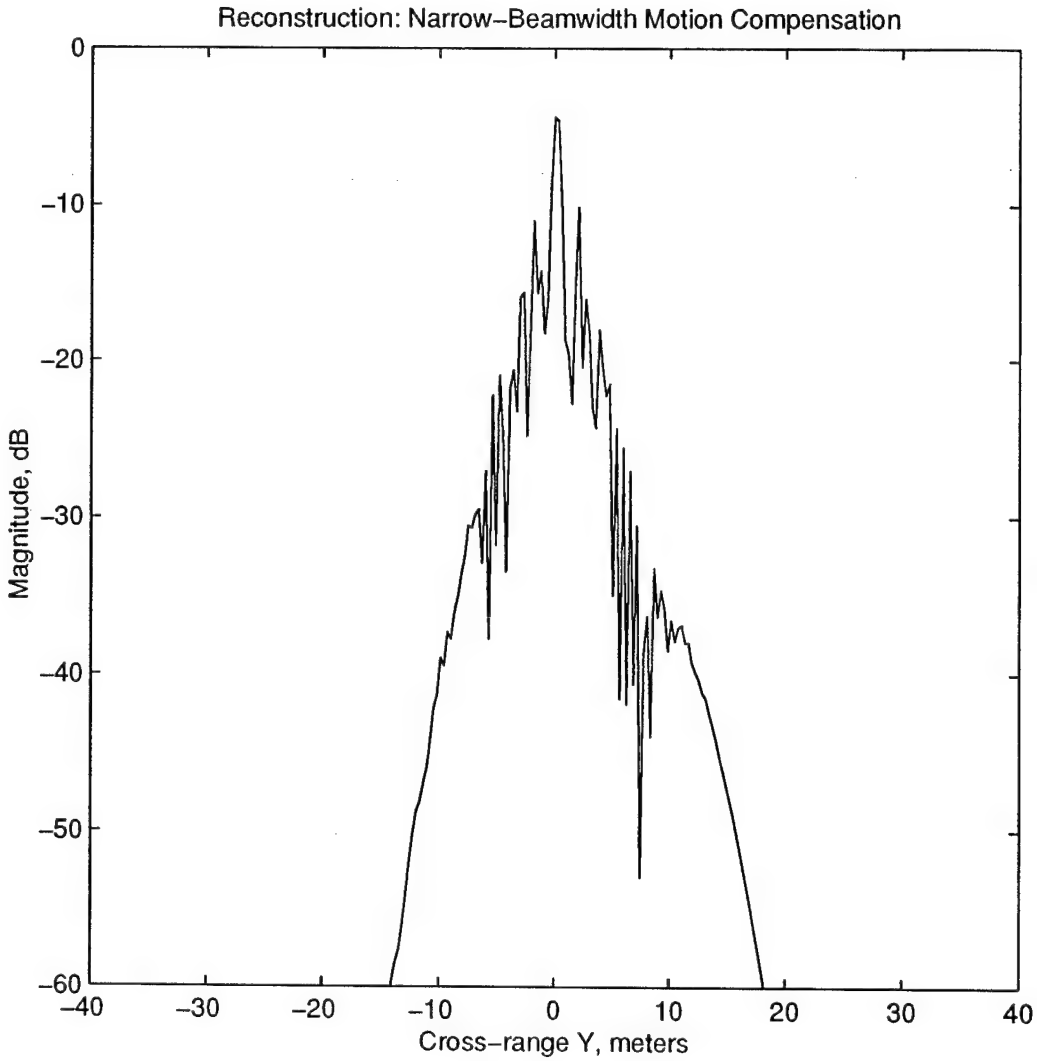
Reconstruction: Narrow–Beamwidth Motion Compensation
Magnitude, dB
0
–10
–20
–30
–40
–50
–60
–40
–30
–20
–10
0
10
20
30
40
Cross–range Y, meters

Figure 4d

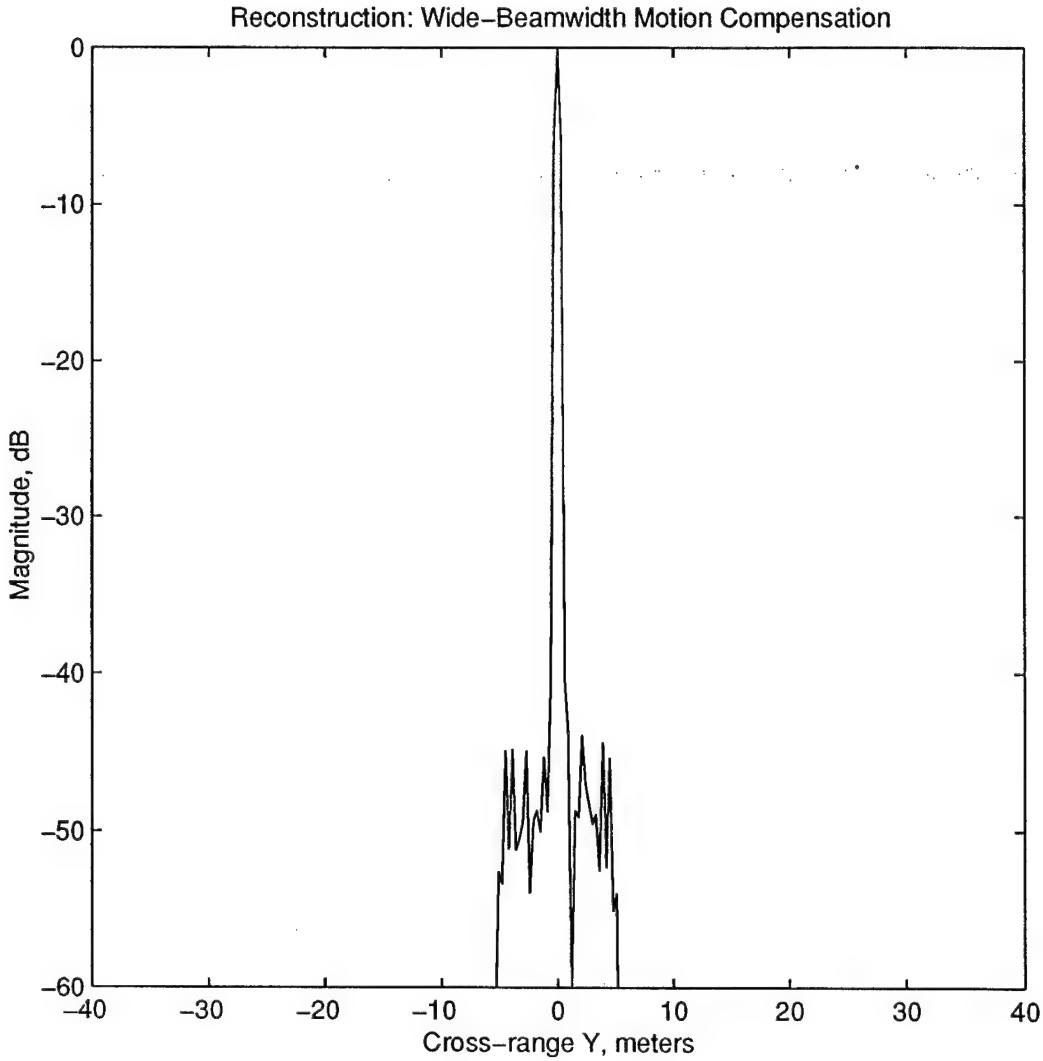
Reconstruction: Wide–Beamwidth Motion Compensation
Magnitude, dB
0
–10
–20
–30
–40
–50
–60
–40
–30
–20
–10
0
10
20
30
40
Cross–range Y, meters

Figure 4e

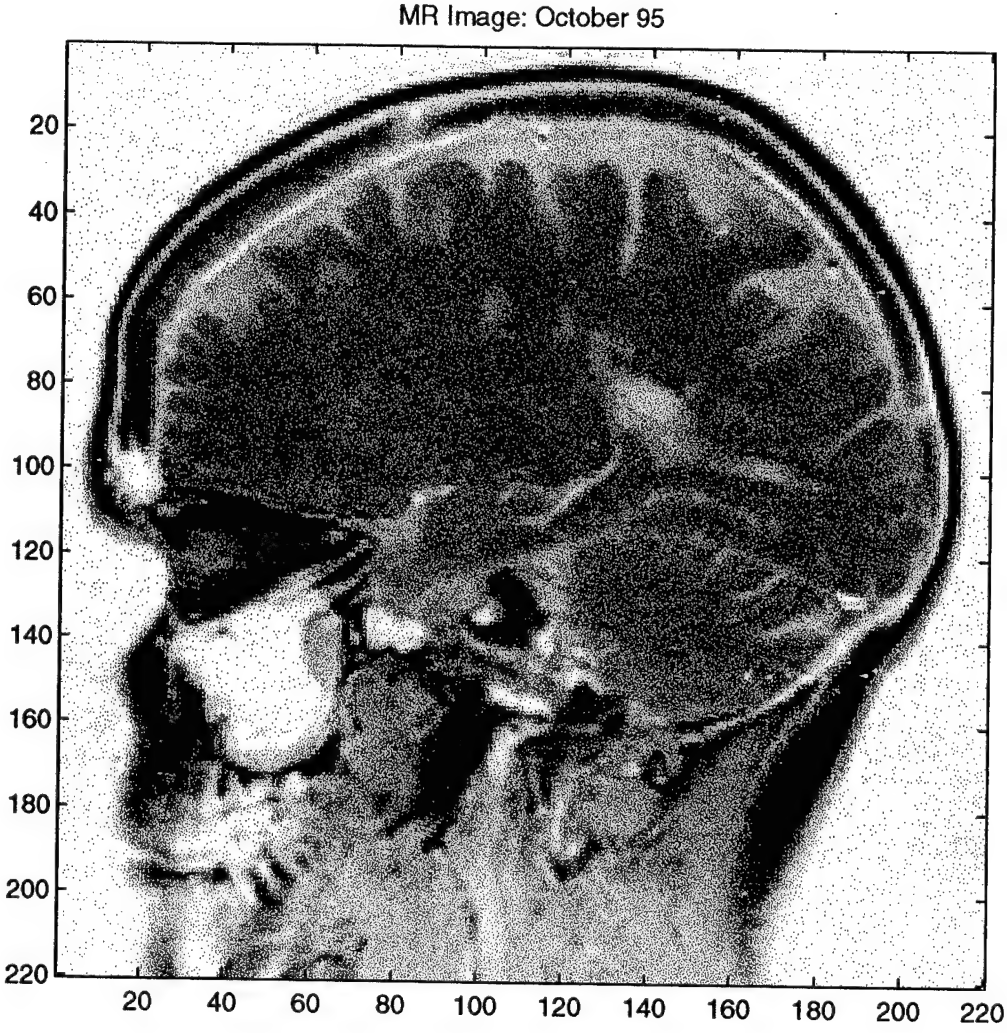
MR Image: October 95
20
40
60
80
100
120
140
160
180
200
220
20
40
60
80
100
120
140
160
180
200
220

Figure 5a

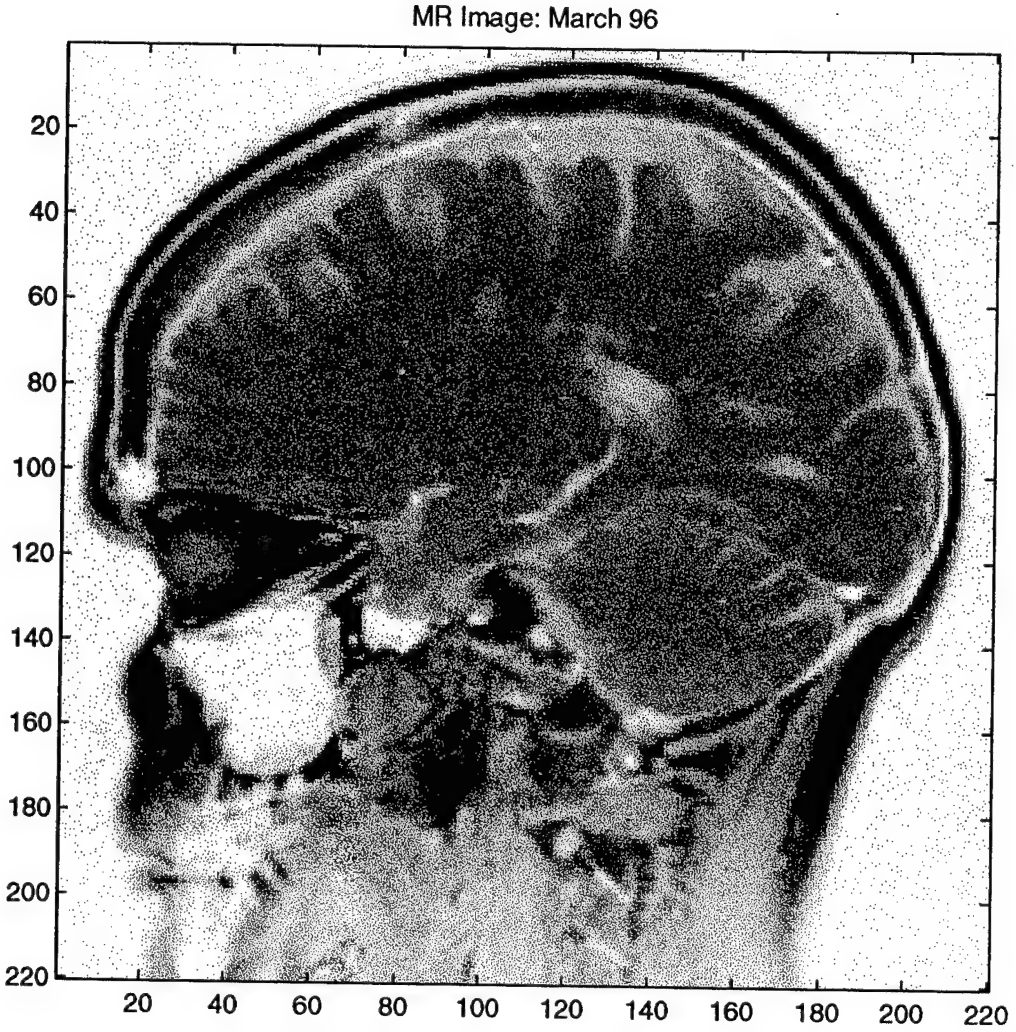
MR Image: March 96
20
40
60
80
100
120
140
160
180
200
220
20
40
60
80
100
120
140
160
180
200
220

Figure 5b

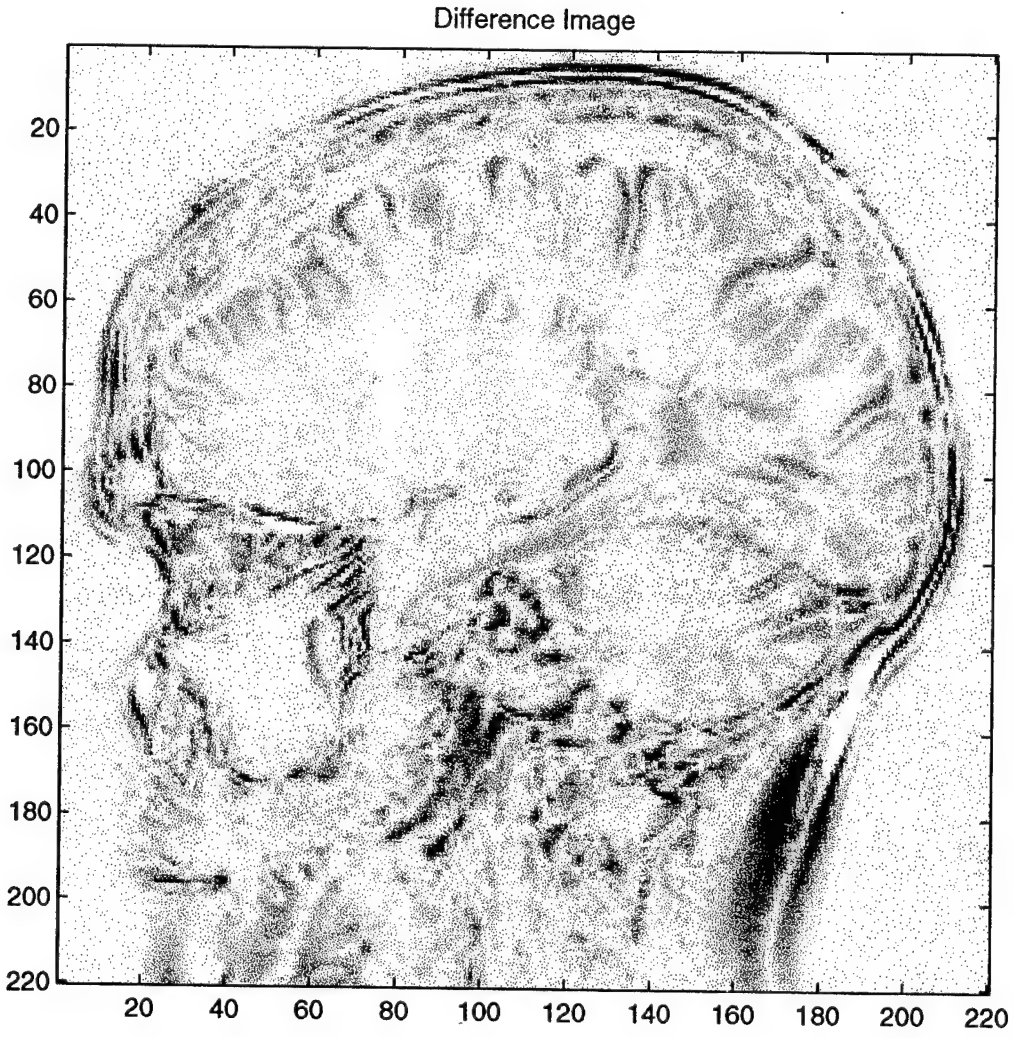
Difference Image
20
40
60
80
100
120
140
160
180
200
220
20
40
60
80
100
120
140
160
180
200
220

Figure 5c

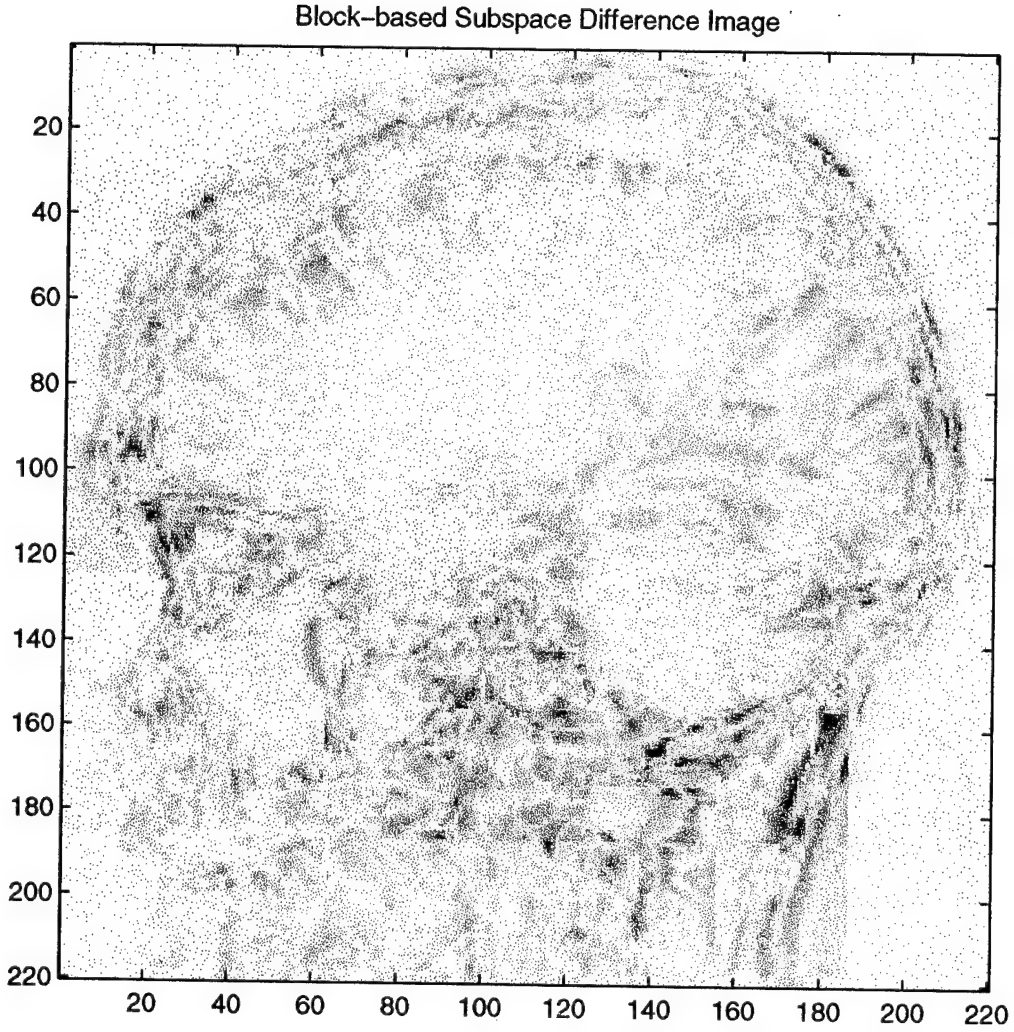
Block-based Subspace Difference Image
20
40
60
80
100
120
140
160
180
200
220
20
40
60
80
100
120
140
160
180
200
220

Figure 5d

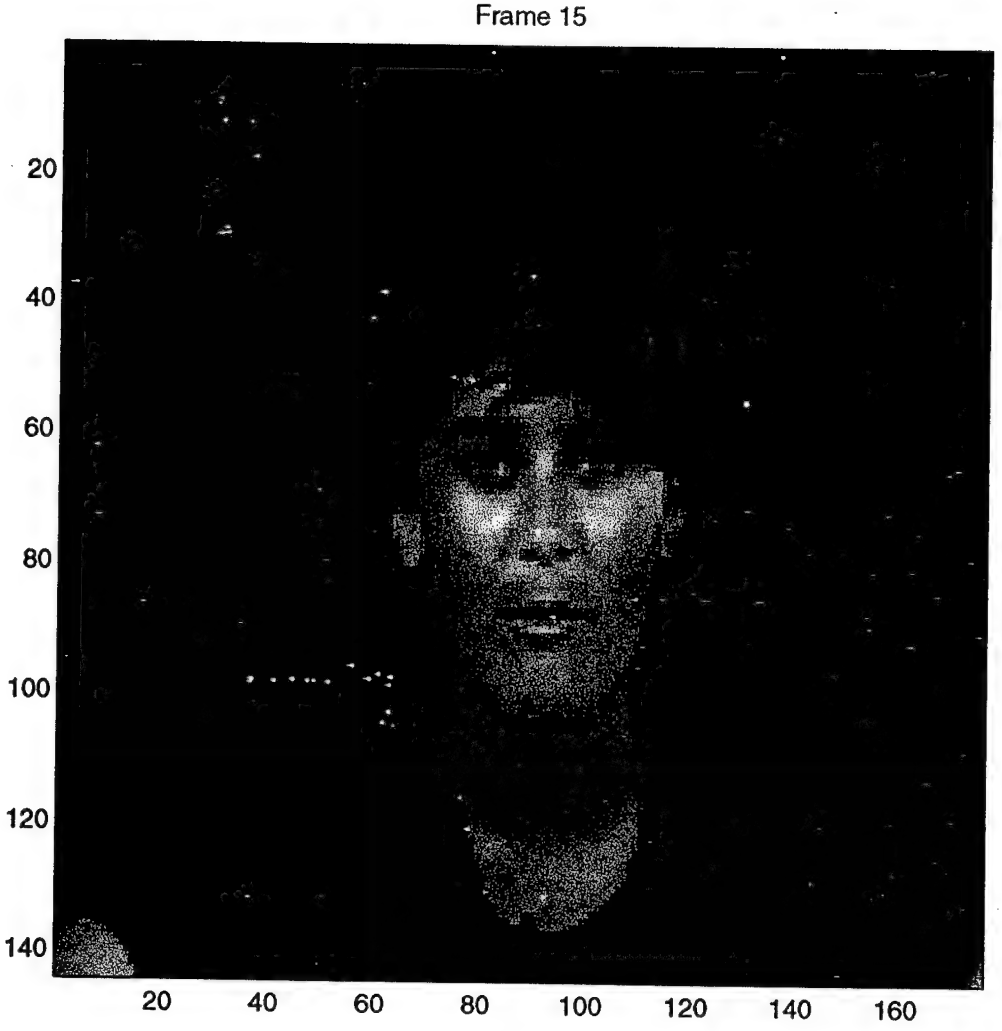

Figure 6a

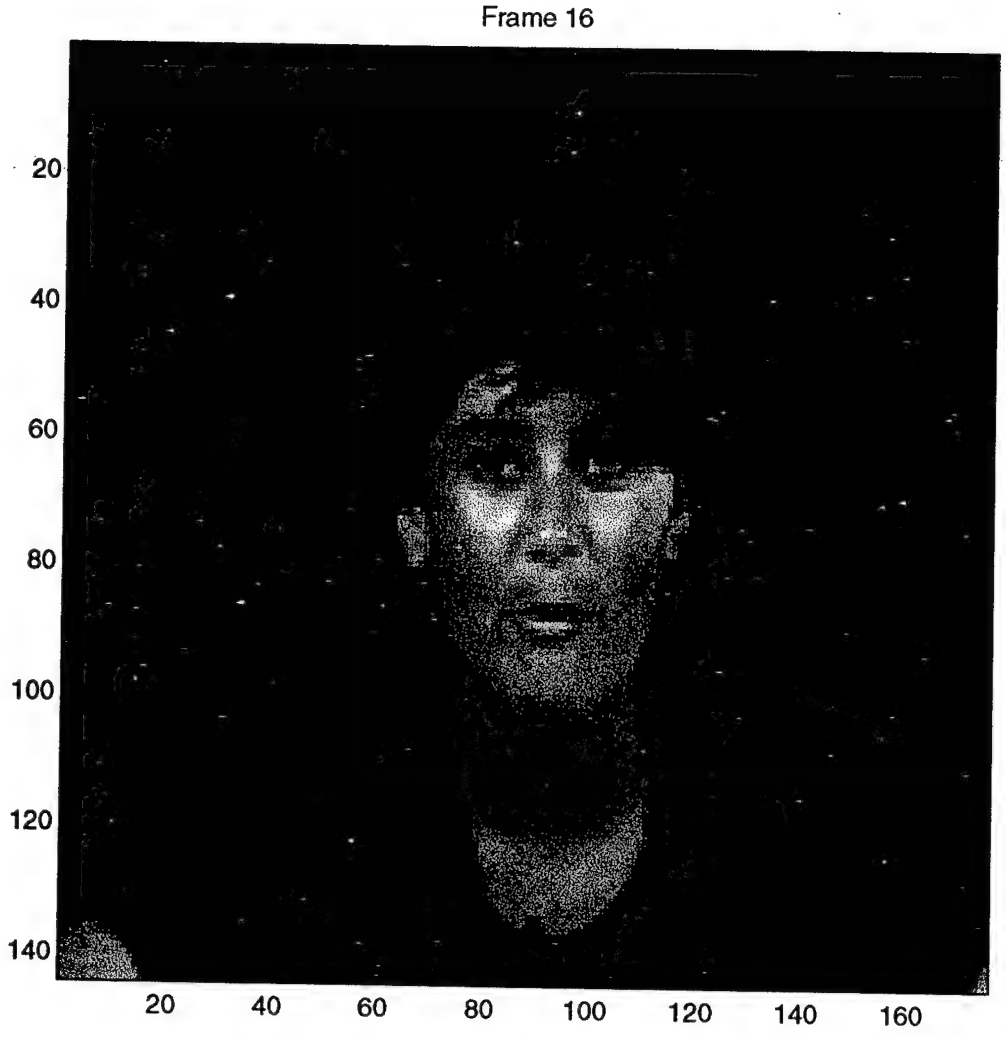

Figure 6b

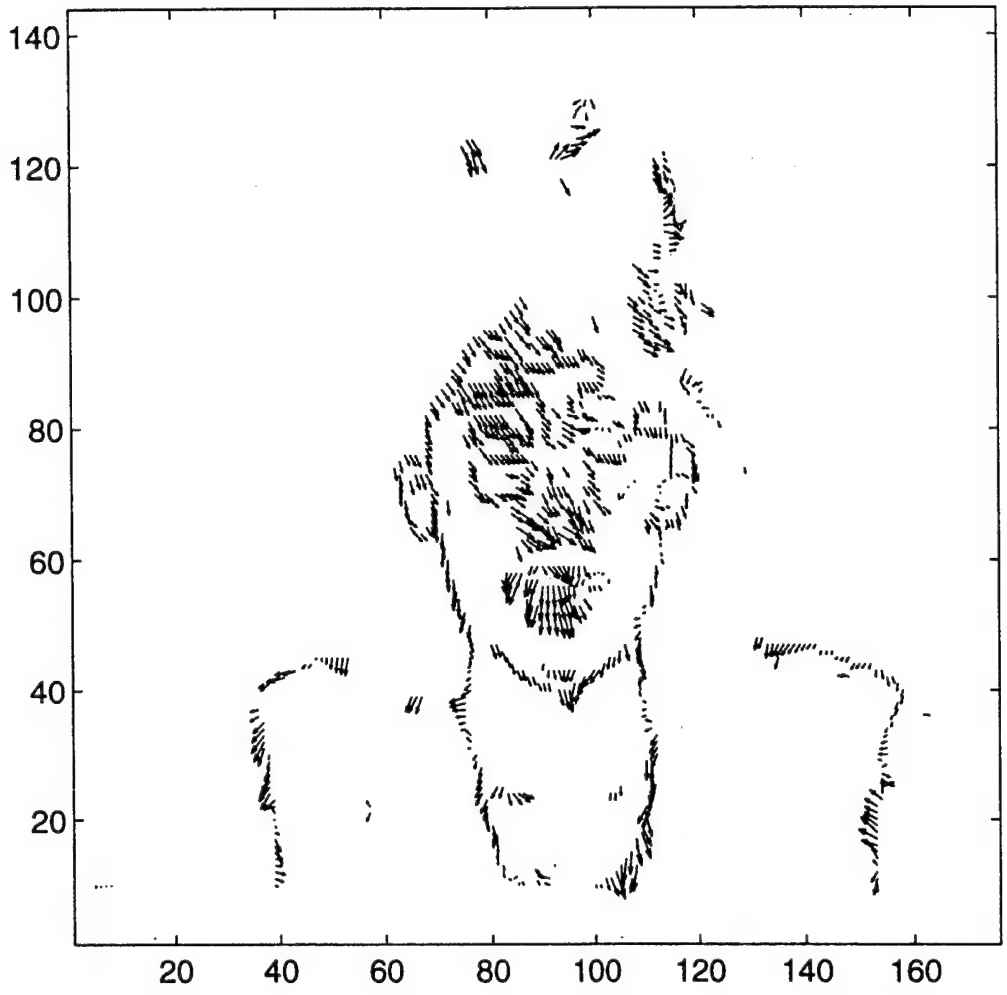

Figure 6c

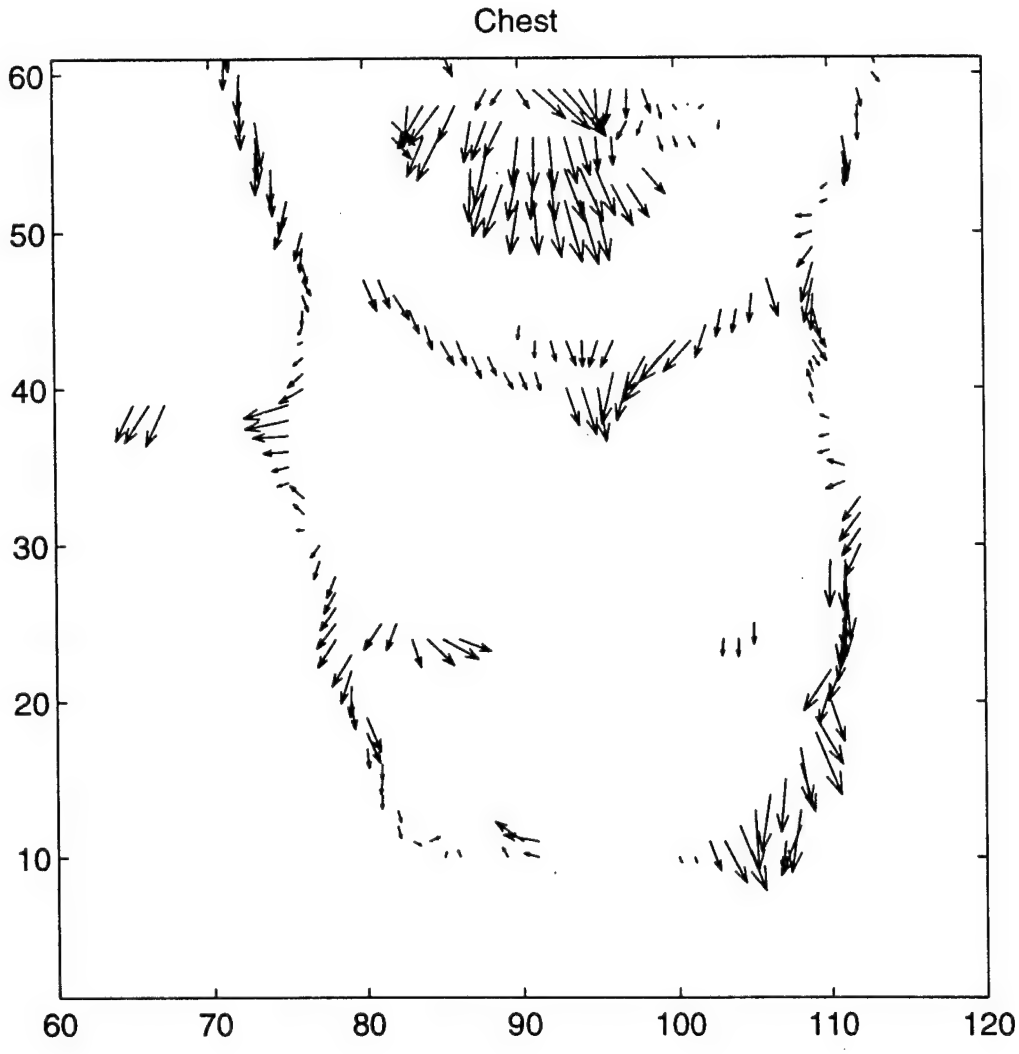

Figure 6d

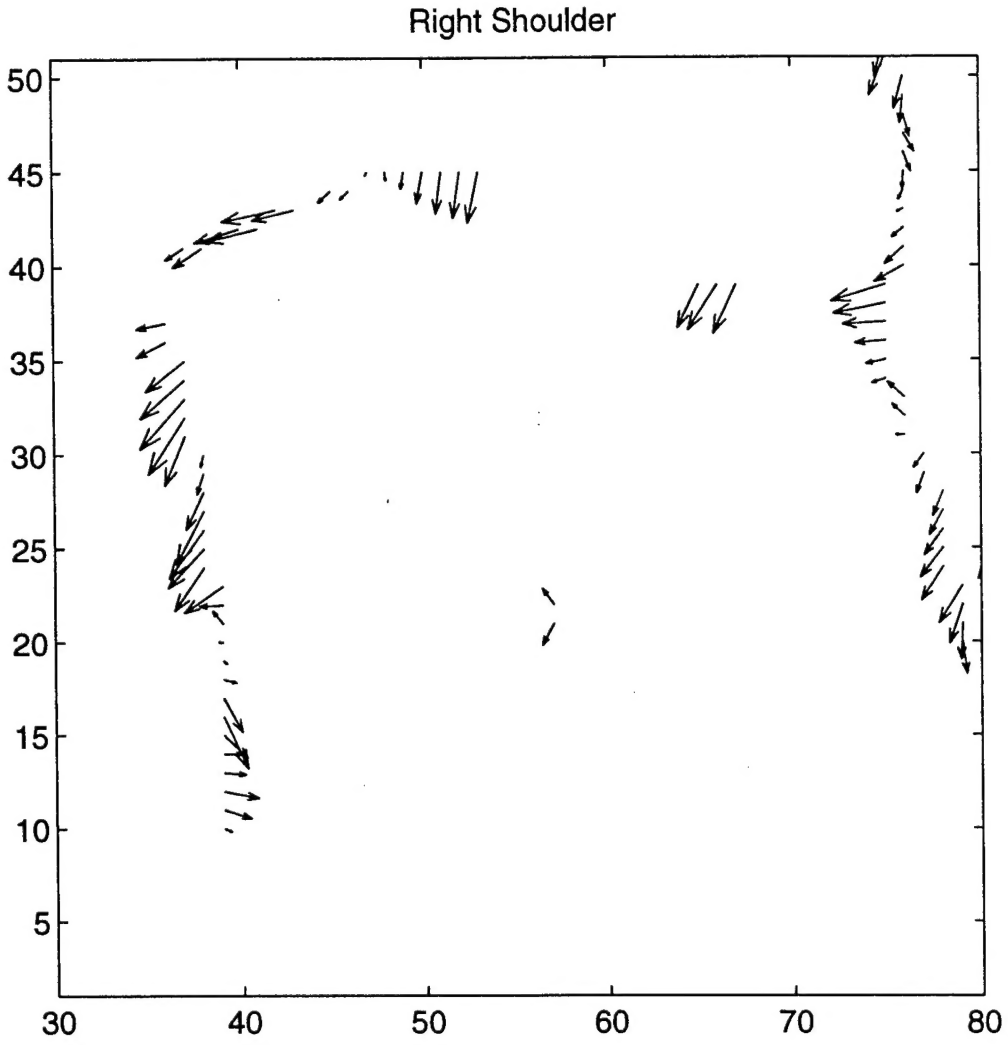

Figure 6e

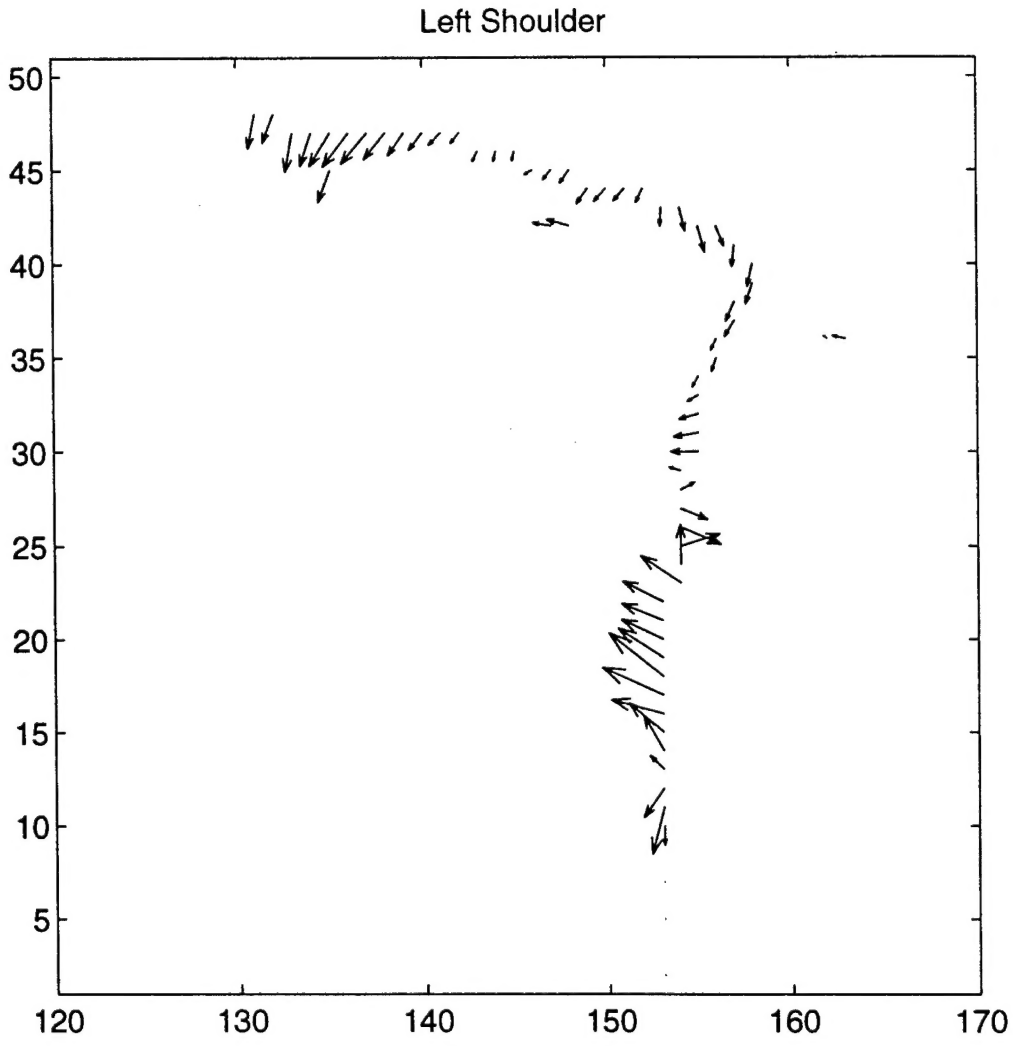

Figure 6f

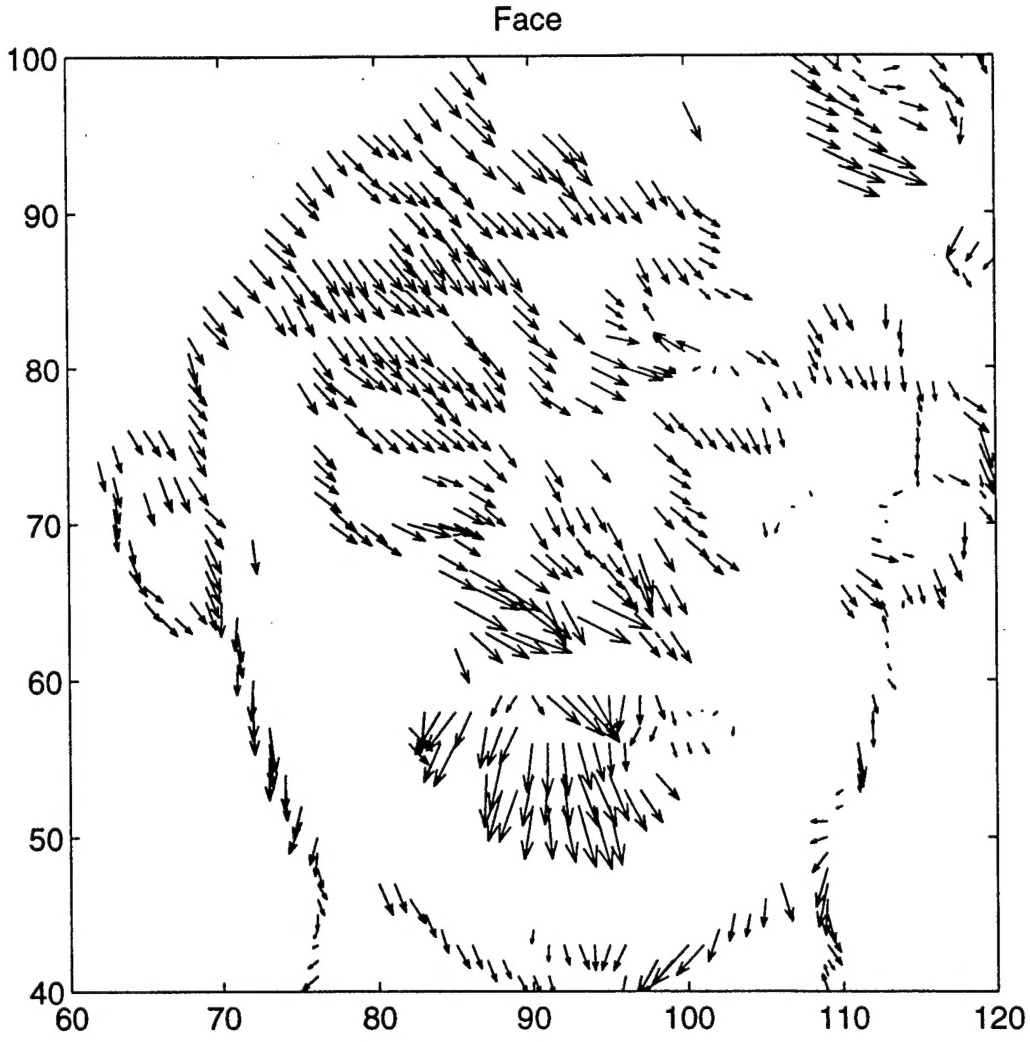

Figure 6g

REPORT DOCUMENTATION PAGE

Form Approved
OMB No. 0704-0188

1. AGENCY USE ONLY (Leave blank)	2. REPORT DATE	3. REPORT TYPE AND DATES COVERED
	9/9/1997	Interim; 10/1/96-9/30/97

4. TITLE AND SUBTITLE
Moving target detection and motion estimation in foilage using along track monopulse synthetic aperture radar imaging; Signal subspace processing of uncalibrated SARs

5. FUNDING NUMBERS
N00014-96-1-0586
N00014-97-1-0966

6. AUTHOR(S)
Mehrdad Soumekh

7. PERFORMING ORGANIZATION NAME(S) AND ADDRESS(ES)
Research Foundation of SUNY-Buffalo
Office of Sponsored Programs Administration
The UB Commons, Suite 211, 520 Lee Entrance
Amherst, NY 14228-2567

8. PERFORMING ORGANIZATION REPORT NUMBER

9. SPONSORING/MONITORING AGENCY NAME(S) AND ADDRESS(ES)
Office of Naval Research Regional Office Boston
495 Summer Street, Room 103
Boston, MA 02210-2109

10. SPONSORING/MONITORING AGENCY REPORT NUMBER

11. SUPPLEMENTARY NOTES

12a. DISTRIBUTION/AVAILABILITY STATEMENT
Approved for public release.

12b. DISTRIBUTION CODE

13. ABSTRACT *(Maximum 200 words)*

Signal subspace processing issues associated with uncalibrated along-track SARs for Moving Target Detection (MTD) and motion estimation are examined. A non-overlapping block-based implementation of the signal subsoace algorithm for MTD and ATR is developed. Overlapping block-based signal subsapce processing to estimate target motion parameters is studied. Application of the signal subspace method in other electronic and camera-based imaging systems, for example, diagnostic medicine and video, are investigated. Calibrating wide-beamwidth monopulse SARs is studied. Numerical results are provided.

14. SUBJECT TERMS
Along-track monopulse SAR; uncalibrated radars; signal subspace processing

15. NUMBER OF PAGES
30

16. PRICE CODE

17. SECURITY CLASSIFICATION OF REPORT	18. SECURITY CLASSIFICATION OF THIS PAGE	19. SECURITY CLASSIFICATION OF ABSTRACT	20. LIMITATION OF ABSTRACT
Unclassified	Unclassified	Unclassified	